01 Apr 2004

An Electromagnetic Model for Evaluating Temporal Water Content Distribution and Movement in Cyclically Soaked Mortar

Shanup Peer

K. E. Kurtis

R. Zoughi
Missouri University of Science and Technology, zoughi@mst.edu

Recommended Citation

S. Peer et al., "An Electromagnetic Model for Evaluating Temporal Water Content Distribution and Movement in Cyclically Soaked Mortar," *IEEE Transactions on Instrumentation and Measurement*, vol. 53, no. 2, pp. 406-415, Institute of Electrical and Electronics Engineers (IEEE), Apr 2004.
The definitive version is available at https://doi.org/10.1109/TIM.2003.822720

An Electromagnetic Model for Evaluating Temporal Water Content Distribution and Movement in Cyclically Soaked Mortar

Shanup Peer, *Member, IEEE*, Kimberly E. Kurtis, and Reza Zoughi, *Senior Member, IEEE*

***Abstract*—Evaluation of water distribution and its temporal movement in cement-based materials is important for assessing cement hydration, curing, and long-term performance. From a practical standpoint, it is also important to obtain this information nondestructively. Near-field microwave nondestructive evaluation methods have proven effective for evaluation of cement-based materials for their various mixture properties, including the detection of salt added to the mixing water and chloride ions entering these materials through exposure to salt water solutions. Electromagnetic modeling of the interaction of microwave signals with moist cement-based materials can provide the necessary insight to evaluate water content distribution and movement in these materials. To this end, the temporal microwave reflection properties of a mortar cube, subjected to cycles of wetting and drying, were measured at 3 and 10 GHz using open-ended rectangular waveguides for several cycles, each lasting about 35 days. A semiempirical electromagnetic model, based on modeling the cube as a layered structure with each layer having a different dielectric constant, was then developed to simulate the measured reflection properties. The simulated and measured results were obtained for both frequencies and, for all cycles, were in good agreement. The most important outcome of the model is the temporal behavior of water content distribution and, hence, its movement in the mortar cube. This paper presents a brief description of the measurement approach and a detailed description of the model. A detailed discussion of the results and its sensitivity to various parameters is also provided.**

***Index Terms*—Concrete, microwaves, moist substances, nondestructive testing, water distribution.**

I. Introduction

INTERACTIONS between cement-based materials and water are important for both strength development (i.e., cement hydration) and performance. Thus, the development of a nondestructive technique to monitor changes in moisture content in cement-based materials is expected to find broad applications. For instance, during initial hydration, such a tool would be useful for verifying water-to-cement ratio (*w/c*). After placement, this tool could also be used to ascertain when a particular degree of hydration has been reached, allowing forms to be removed at an appropriate time, or to monitor moisture loss to the environment as a means of assessing the likelihood of cracking. During service, ingress of moisture, which can be accompanied in some environments by potentially aggressive ions and gases (e.g., Cl^-, SO_4^{2-}, CO_2), could be monitored to provide information regarding the degree of saturation and depth of penetration. Thus, such a tool could form the basis for service life predictions and maintenance strategies where reactions involving moisture ingress (e.g., alkali-silica reaction, carbonation, corrosion, freeze-thaw cycling, and sulfate attack) are expected [1]–[4].

Therefore, accurate evaluation of moisture ingress and its gradient of penetration into cement-based materials are important practical issues to those interested in health monitoring of concrete structures. A reliable and accurate, but painstaking, technique to determine the moisture profile would be to core and slice the cubes during each day of every drying cycle at various depths and make gravimetric measurements to determine the temporal water content as a function of depth into the cube for each day of the cycle. However, this would require numerous cubes to be subjected to similar wetting and drying cycles. Assuming that identical conditions exist within all the cubes, each cube could then be cored and sliced to obtain the temporal water content for one particular day. It is important to note that once a cube is cored, it would be rendered useless for the rest of the investigation. The practical difficulties that arise from this technique make it desirable to perform such an evaluation nondestructively. Several nondestructive evaluation techniques have been used to monitor moisture movements in cement-based materials, including magnetic resonance imaging (MRI), nuclear magnetic resonance, neutron scattering, and gamma-ray densimetry [1], [2], [5]–[7]. Near-field microwave nondestructive evaluation methods have previously shown to be effective for evaluation of mixture proportions and chloride ingress in cement-based materials [8]–[27].

Here, the utility of these near-field microwave nondestructive evaluation techniques to accurately evaluate moisture distribution and movement in cement-based materials will be assessed. To this end, a mortar cube was exposed to cyclical episodes of soaking and drying. Subsequently, the temporal microwave reflection properties of the cube were measured at 3 and 10 GHz for several cycles. This paper presents a brief description of the measurement approach and a detailed description of a semiempirical electromagnetic model simulating the measured results. Finally, a complete discussion of the results will be presented.

Manuscript received December 16, 2002; revised October 6, 2003. This work was supported by The National Science Foundation under Grant NSF CMS-0196158. Any opinion, findings, and conclusions or recommendations expressed in this material are those of the authors and do not necessarily reflect the views of the National Science Foundation.

S. Peer and R. Zoughi are with the Applied Microwave Nondestructive Testing Laboratory (AMNTL), Electrical and Computer Engineering Department, University of Missouri-Rolla, Rolla, MO 65409 USA.

K. E. Kurtis is with the School of Civil and Environmental Engineering, Georgia Institute of Technology, Atlanta, GA 30332 USA.

Digital Object Identifier 10.1109/TIM.2003.822720

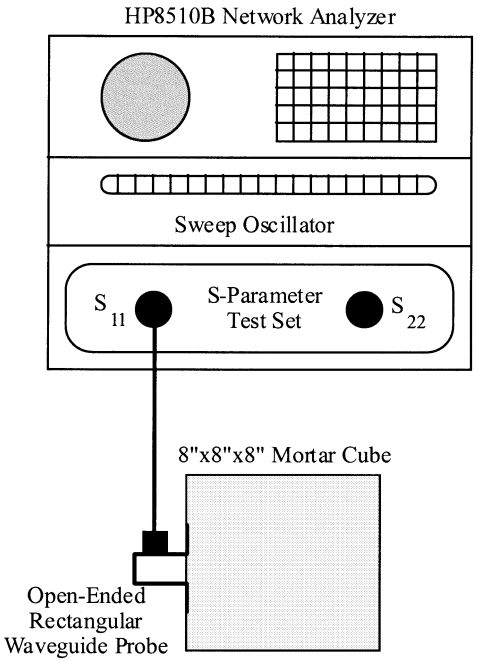

Fig. 1. Measurement apparatus.

II. Experimental Methodology

A. Sample Preparation and Exposure

A $200 \times 200 \times 200$ mm $(8'' \times 8'' \times 8'')$ mortar cube having a *w/c* of 0.50 and a sand-to-cement ratio (*s/c*) of 2.5 was produced using tap water and portland cement type I/II [26], [27]. The cube was then placed in a hydration room for 24 h and, subsequently, left at room temperature and low humidity for another ten months. The cube was then submerged to within $\sim$ 6 mm $(\sim 1/4'')$ of its top surface in a distilled water bath 20 h during each wetting cycle. The cube was subsequently removed from the bath and left in ambient conditions for 24 h to allow the water on the surface of the cube to evaporate before the microwave measurements were conducted.

B. Measurement Approach

During the next 35 days (i.e., the drying cycle), using open-ended rectangular waveguide probes in conjunction with an HP8510B vector network analyzer as shown in Fig. 1, the daily microwave reflection properties of this cube were measured at two different frequency bands, namely S-band (2.6–3.95 GHz) and X-band (8.2–12.4 GHz). To obtain an average value of the reflection properties, 16 measurements were performed on the cube (four per side) at S-band, while 36 measurements (nine per side) were made at X-band (the rectangular waveguide probe apertures is smaller at the latter frequency band). This procedure was repeated for three such wetting and drying cycles. It has been reported that the drying period is an important factor in moisture ingress into cement-based materials [3]. Concurrently, the mass of the cube was also measured on a daily basis and this information was later incorporated into the electromagnetic model as the only physical data. The measured results are reported and the modeling analyzes are performed for two specific frequencies of 3 GHz (S-band) and 10 GHz (X-band), representing each frequency band.

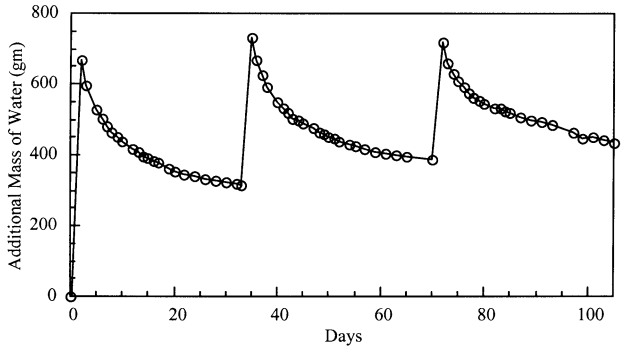

Fig. 2. Daily mass of water in the cube for the three cycles.

III. Experimental Results

When soaked, water penetrates into the mortar through interconnected pores and cracks through a combination of absorption, diffusion, dispersion, permeation, and wicking [3]. Once removed from the water bath, a portion of the water evaporates over time from the near surface regions (i.e., first few millimeters). If the mortar is not completely saturated through its depth during the wetting period, some of the water remaining in the near-surface regions continues to be drawn toward the drier regions closer to the sample core. Unless the cube is subjected to oven drying after each soaking cycle, some water will remain in the voids and pores, and the moisture content will vary from the surface to the core.

The mass of the cube was measured to coincide with the microwave measurements. Because of the age of the mortar, it may be presumed that changes in mass can be related to moisture uptake or loss. Loss in mass due to leaching has been neglected. Fig. 2 shows the change in mass in the cube for the three soaking cycles, indicating the gain in mass of the cube relative to its mass on day zero (i.e., the pre-soaked mass). The results also show an increase in the mass of the cube at the end of each cycle with respect to the end of previous cycle. This indicates an amount of residual water in the cube prior to the next soaking. Because of the age of the mortar prior to soaking (i.e., greater than ten months), it is not expected that an increase in mass would reflect continued hydration. Additionally, relative to the moisture uptake due to soaking, the prior-to-soaking moisture in the cube, if any, was assumed to be significantly less and nonexistent in the context of the modeling approach.

The calibrated effective reflection coefficient of the cube is a complex parameter consisting of a magnitude and a phase for a specific frequency. The reflection property of the cube (e.g., considered a half-space for these measurements [14], [15]) for a given frequency is a function of its effective complex dielectric properties of the cube. Effective refers to the fact that the dielectric properties of the cube vary from its surface toward its core as the drying progresses, since the water distribution within it continually changes. When soaked, water fills some of the pores. Thus, soaked mortar comprises of a base or host material (i.e., mixture of hardened cement paste and sand) and air and water as the two primary inclusions. Therefore, the effective complex dielectric properties of mortar are dependent upon the volume fraction and the individual dielectric properties of the host and its inclusions and their distribution throughout the cube.

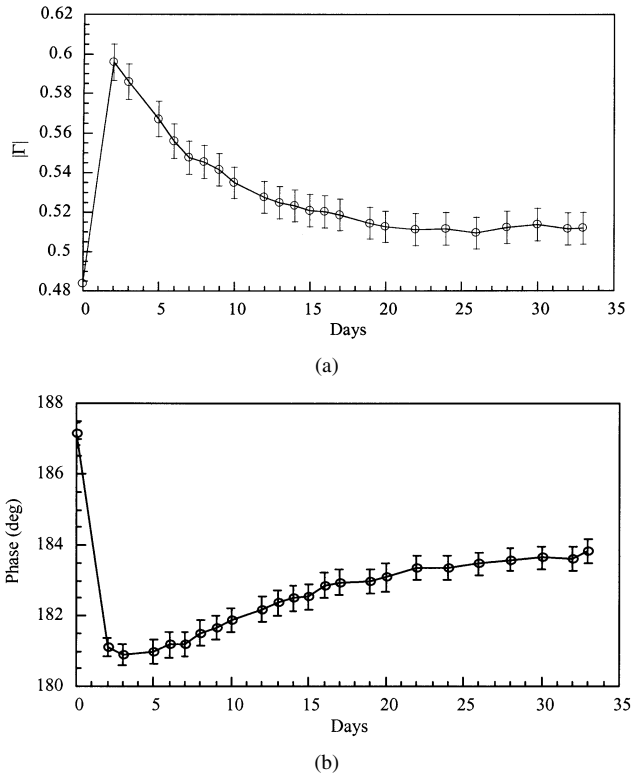

Fig. 3. (a) Magnitude and (b) phase of reflection coefficient at 3 GHz for cycle 1.

The process of evaporation begins as soon as the cube is taken out of the water bath. As the water evaporates, the effective dielectric properties of the cube, which depend on the volume fraction of water present in the cube, change, and, hence, the effective reflection coefficient of the cube changes on a daily basis, as well. This issue will be further discussed in the modeling section. Fig. 3(a) and (b) shows the daily measured magnitude ($|\Gamma|$) and phase of reflection coefficient of the cube for the first soaking cycle at 3 GHz. The circles represent the average values while the vertical bars represent the standard deviation. Day zero results refer to the day prior to the soaking of the cube. The results show a continuous reduction in $|\Gamma|$ as a function of increasing days, primarily indicating the evaporation of water from the cube. The increase in the measured phase of reflection coefficient also indicates a similar phenomenon [26], [27]. However, the overall behavior of $|\Gamma|$ and phase at each frequency is indicative of a more complex phenomenon involving the temporal distribution of water and its movement within the cube.

IV. Modeling Approach

A. Modeling Considerations

As described in Section II-B, for each frequency band, several reflection property measurements were conducted on four sides of the cube. By using the resulting average value of $|\Gamma|$ and phase at each frequency, the spatial properties of the cube across its sides can now be considered to be uniform and the only variation in properties is along the distance into the cube. Therefore, the water distribution within the cube is now assumed to vary only as a function of the distance into the cube (i.e., depth from the cube surface). Subsequently, a multilayered formulation for obtaining the reflection properties of a layered structure [28], as shown in Fig. 4 was considered. This formulation gives the magnitude and phase of reflection coefficient, measured by an open-ended rectangular waveguide probe, for a stratified dielectric material at a specified frequency, number of layers n and thickness t_n, and the (relative to free-space) dielectric properties of each layer ε_{rn}. This existing, versatile, and well-tested formulation provides for several unique features that are important for the modeling of water movement in cement-based materials, namely as follows.

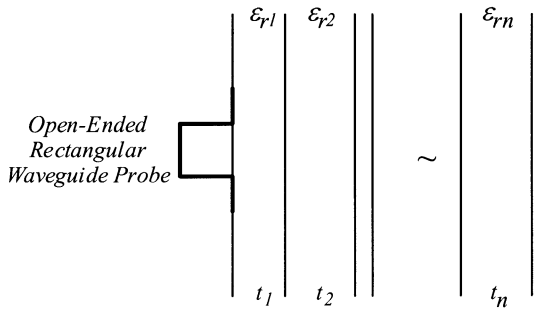

Fig. 4. Schematic of an open-ended rectangular waveguide probe radiating into an arbitrary layered dielectric structure.

- As per the experimental approach, it describes the interaction of an open-ended rectangular waveguide probe with a layered structure.
- The dielectric properties of each layer needed as input to the model are directly related to the dielectric properties and volume content of the host (i.e., mortar) and the inclusions (i.e., water) in each layer. Therefore, the results will be directly dependent on the volume content of water in each layer resulting in the sought-for water content distribution within the cube. Additionally, as a function of days, the water content in each layer changes and hence the overall results will also indicate the manner by which water is distributed or *moves* within the cube during the drying cycle.
- The cube can be modeled to have as many number of layers as necessary. This in an important issue since the thinner the layers are the more accurate the water content distribution within the cube can be evaluated. It has also been suggested that for the purpose of water movement evaluation in cement-based materials (e.g., transport of aggressive ions), the water content must be evaluated or resolved in these materials with fine (i.e., millimeter or sub-millimeter) resolution [1].
- The dielectric properties of each layer can be calculated using a number of dielectric mixing models [29]. Dielectric mixing models give the effective dielectric properties of a mixture composed of a host material (i.e., mixture of hardened cement paste and sand) and several constituents (i.e., air and water) as a function of the dielectric properties and volumetric content of the host and the inclusions. The dielectric properties of hardened cement paste, sand and water are known at 3 and 10 GHz [8], [9], [11], [12], [29], [30]. Previously developed mixing models for mortar can also be used to reasonably closely determine its porosity

[11], [12]. Therefore, the temporal water content in each layer entering and leaving the pores becomes an important parameter in the model yielding temporal water content distribution within the cube.

When the soaked cube is analyzed or modeled as a collection of discrete layers, it is quite obvious that each of the layers would have varying water content. Consequently, the amount of water that evaporates from each layer is dependent on its relative distance from the surface of the cube. The information provided by the measured daily mass of the cube, as shown in Fig. 2, provides for the total daily amount of evaporated water, as well as the amount of water remaining in the cube, as compared to its water content on day 0, at any given time. It is important to note that Fig. 2 does not provide any information regarding the daily water distribution in the cube. However, the information regarding the temporal contribution of each layer to the amount of water that evaporates from the cube, as well as the amount of water present in the layers can be obtained through the modeling process presented in this paper.

Additionally, due to various other phenomena (such as absorption, diffusion, permeation, wicking, and capillary draw), moisture also moves between the layers. Hence, to be able to predict the temporal water content in each layer, it is necessary to model not only the amount of water that is lost by each of the layers due to evaporation, but also the amount of water that *moves* among the layers. Once such a model is developed, it then becomes imperative to have proper comparison standards to ascertain the accuracy of the simulation results. From an electromagnetic perspective, this can be achieved by measuring the reflection properties of the cube at various frequency bands on a daily basis. The validity of the model can then be evaluated from a comparison between the measured and the simulated results at different frequency bands. That is why, for the purpose of this investigation, the temporal microwave reflection properties of the cube were measured at S-band and X-band for each of the three cycles. Additionally, these two frequency bands have shown great promise for evaluating the various properties of cement-based materials [11], [12], [14], [15], [21].

An important point to be mentioned is that the frequencies constituting S-band range between 2.6 and 3.95 GHz, while those constituting X-band vary between 8.2 and 12.4 GHz. Consequently, microwave signals in the S-band frequency range penetrate relatively deeper into the mortar cube, as compared to the signals at the X-band frequency range. Water also possesses much higher dielectric properties, in particular, a higher loss factor than the rest of mortar constituents. Therefore, during the first few days following soaking, X-band frequencies are capable of penetrating only up to a few millimeters into the cube, while S-band frequencies may penetrate tens of millimeters into the cube. Hence, X-band (10 GHz) results essentially provide near surface information while S-band (3 GHz) results provide information about deeper regions into the cube. This feature is important when trying to modify the model parameters (i.e., empirical parameters) for a more accurate simulation of the measured results. Consequently, this fact aids in better evaluation of water content distribution in the cube.

Thus, to evoke this multilayered formulation at a given frequency and for each day of each cycle, the number of layers, their individual thickness, and dielectric properties must be known. The following sections describe this modeling process and steps taken to better modify these input parameters over the course of its development.

B. Modeling Procedure

The most important initial parameter that is needed for the development of the model is the conceptualization of the water distribution inside the cube. At the outset, several water distribution functions were employed to simulate the reflection properties of the cube on a daily basis rendering no encouraging results. In hindsight, the primary shortcoming of these distribution functions was the fact that they could only model evaporation of water (on a day-to-day basis), which, as discussed earlier and will be seen later, is not the only phenomenon occurring inside the cube. Additionally, through these investigations, it became evident that to simulate the shape/trend of the phase of reflection coefficient, particularly during the first few days of a cycle, it was not sufficient to use water distribution functions that progressively decreased in amplitude as a function of days (i.e., representing evaporation only). To gain an understanding of the water content distribution that might exist within the cube, an initial model was developed [31]. The salient features of the model involved a) estimation of the depth of penetration of the microwave signal into the cube at several discrete frequencies in the S-band and X-band frequency range using a plane-wave approximation [25], b) evaluation of the volume fraction of water up to the effective depth of penetration of the signal at each of these frequencies, and c) correlation of the effective penetration depth and volume fraction of water at each of the discrete frequencies. The results suggested that the relative moisture content inside the cube progressively increases with increasing depth from the surface of the cube until it reaches a maximum value at some depth after which it then decreases toward the core of the cube. Rayleigh-like functions possess such overall shapes. Consequently, the following general equation for the water content distribution function $(\mathrm{WCD}(t))$ was employed in this model:

$$\mathrm{WCD}(t) = k_4 \left[\frac{t}{k_1}\right]^{k_2} e^{\left[-k_3\left(\frac{t}{k_1}\right)^{k_2}\right]} \quad (\mathrm{gm/mm}) \qquad (1)$$

where t is the thickness which varies from the surface of the cube to its center (i.e., 0 to 100 mm), k_1, k_2, and k_3 are empirical parameters, and k_4 is the maximum value (amplitude) of the distribution function for each day. The empirical parameters k_1, k_2, and k_3 change as a function of days and were obtained from a rigorous trial and error method by matching the simulation with the measured reflection coefficient results. As will be explained in detail later, Fig. 5 shows a family of distribution functions using (1) for nine days of cycle 1.

Now, for each day, the integral of these functions must match the total mass of water in the block for that day (Fig. 2). As mentioned earlier, the only ground truth data that is an input to this model is the daily mass of the cube, although k_1, k_2, and k_3 for each day are obtained by comparison of the simulation and the measured reflection coefficient results. The cube was soaked in the water bath in such a way that its top surface was

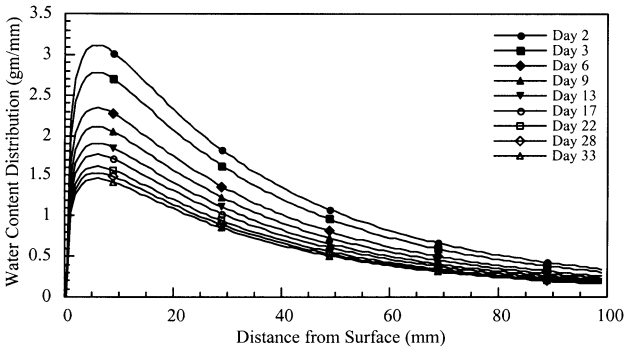

Fig. 5. Water content distribution obtained from the model, with only evaporation accounted for, for cycle 1.

below the water line by $\sim$ 6 mm ($\sim 1/4''$). During the drying cycles, the cube was raised $\sim 1''$ from the holding table to allow evaporation from all six surfaces. However, the amount of water that evaporates from the top and bottom sides is expected to be less than the other four sides. Recall that the microwave measurements were conducted at four sides only (excluding the top and bottom sides). Hence, to account for this nonuniformity, the daily mass (see Fig. 2) of the cube was subtracted from the pre-soaked mass and then this value was divided by five indicating an effective water content seen by the microwave signal from each side. In this way, the moisture distribution is assumed to be uniform across the cube sides and only varies as a function of depth according to (1). As mentioned earlier, the uniformity assumption across the cube side surface is justified by the fact that several microwave reflection measurements were conducted across each side and then averaged. Nonetheless, this could also be considered a geometry dependent empirical factor (similar to k_1, k_2, and k_3). The influence of variations in this factor on the simulated daily magnitude and phase of reflection coefficient will be further discussed later. Now that a continuous equation for the water content distribution function is obtained, the modeling process using the multilayered formulation can initiate. The following is the step-by-step procedure for this modeling approach.

Step 1) The daily mass of the cube is subtracted from its pre-soaked value indicating the change in the amount of water in the cube (see Fig. 2). This value is then divided by five, as explained above, and is denoted by m.

Step 2) With k_4 set to 1, the integral of the water content distribution function [i.e., total water (TW)] is calculated over a cube thickness of 100 mm, namely

$$\mathrm{TW} = \int_{t=0}^{t=100} \mathrm{WCD}(t)dt \quad (\mathrm{gm}). \tag{2}$$

Although the thickness of the block $\sim$200 mm, by using a factor of five to divide the mass of water over the cube volume, a uniform distribution of moisture over the four measured sides has been assumed. This integral also represents the total amount of water in the cube absorbed during soaking from one surface up to the center of the cube.

Step 3) Now, k_4 is equal to the ratio of m and TW (i.e., m/TW).

Step 4) The cube is then discretized into 1 mm-thick layers.

Step 5) With the obtained values of k_1, k_2, k_3, and k_4 the integral of the total water content distribution is again found for every 1-mm layer inside the cube, namely

$$\mathrm{TW}(t_1) = \int_{t_1}^{t_1+1} \mathrm{WCD}(t)dt \quad (\mathrm{gm}). \tag{3}$$

The above integral denotes the total amount of water uniformly distributed in every 1-mm-thick layer of the cube.

Step 6) The water distribution in the specimen gives an indication of the porosity of the specimen. As mentioned earlier, each of the layers within the specimen holds varying amounts of water. In this case, each layer is assumed to be 1–mm thick and the amount of water that each of these layers contain is obtained by integrating the moisture content distribution functions for 1 mm (centered at that thickness). The constraint on the upper limit of water content in each layer is set by the porosity of the specimen. If we assume that the thickness at which the peak of the water distribution curves occur (for day 1) is saturated with water, it would then mean that the ratio of the volume of water at that thickness to the volume of mortar for a thickness of 1 mm (200 $\times$ 200 $\times$ 1 mm) would be a fairly reasonable indication of the (average) water-accessible porosity of the specimen. Once the amount of water at that thickness is obtained from the water content distribution functions, it has to be first converted to its equivalent volume (the density of water is 1 g/cc) to determine the ratio. This ratio is then the average porosity of the specimen. Subsequently, a dielectric mixing formula is used to determine the effective dielectric properties of each corresponding layer. There are numerous dielectric mixing formulae available that may be used to evaluate the effective dielectric properties of the soaked mortar mixture [29], [33]. When the inclusion (i.e., air and water) volume fractions are relatively small, as is in this case, most of these formulae render very similar results. Thus, the following simple dielectric mixing formula was used to calculate the complex relative (to free-space) effective dielectric constant $\varepsilon_{\mathrm{reff}}$ of every 1-mm thickness of the mortar cube

$$\varepsilon_{\mathrm{reff}} = \varepsilon_{\mathrm{rw}} f_w + \varepsilon_{\mathrm{rm}} f_m + f_a \tag{4}$$

where $\varepsilon_{\mathrm{rw}}$ and $\varepsilon_{\mathrm{rm}}$ are the complex relative dielectric properties of water and mortar, respectively, and f_w, f_m, and f_a are the volume fractions of water, mortar, and the air in each 1-mm thick layer (i.e., $f_w + f_a = 1 - f_m$).

Step 7) Once the dielectric properties of each of the 100 individual layers of 1-mm thick were obtained, the multilayered formulation to simulate the measured

reflection properties at the waveguide aperture was evoked.

Step 8) k_1, k_2, and k_3 are subsequently obtained from a rigorous trial-and-error process based on matching the simulation results of $|\Gamma|$ and phase to their corresponding measured values.

Step 9) The entire above procedure was then carried out for each day of each cycle.

V. Results

A. Cycle 1

Fig. 5 shows the outcome of the water distribution model obtained through Steps 1–3 for the first cycle of wetting and then drying for several days. These curves are used to simulate the microwave reflection properties of the cube starting from one day after the cube was removed from the bath. The results show several important phenomena. After one day, it is expected that any water immediately at the surface of the cube has evaporated. These curves clearly represent this phenomenon as the net change in water content (as compared to the moisture state of the cube prior to soaking) at the surface of the cube is zero and rapidly increases as a function of distance into the cube. The peak of water content is shown to occur at a depth of $\sim$6 mm from the cube surface and this peak remains at this location for all of the days in the drying cycle. For depths beyond the peak, the distribution for all days drops somewhat rapidly and reaches a small but nonzero value for the last day of the cycle (i.e., day 33) and at a depth of 100 mm inside the cube. This behavior is also intuitive, since it can be assumed that not all of the water evaporates from the cube during the cycle and some water remains in the cube. The curve for day 33 shows the water distribution in the cube for the last day of cycle. The integral of this curve represents the total increase in water present in the cube at day 33, as compared to the moisture state of the cube before soaking. It is important to note that these curves only depict the process of evaporation since the peaks of these curves, as well as their shapes, remain stationary as a function of increasing days and only the amplitude of the curves progressively decreases.

Fig. 6(a) shows the comparison between the simulated and measured $|\Gamma|$ at 3 GHz (S-band) using the water distribution functions shown in Fig. 5 and the steps outlined in the previous section. The results indicate that, other than day 1, the simulated and the measured results do not match well; however, the decreasing trend of $|\Gamma|$ as a function of increasing days is very encouraging. Fig. 6(b) shows the comparison between the simulated and measured phase of reflection coefficient at the same frequency. There are several important facts that need to be discussed when studying the simulated phase results. First, there is a distinct dip in the phase behavior during the first five days that the model fails to predict. As will be shown later, this dip is indicative of the temporal movement of the peaks which, for the distributions shown in Fig. 5, were stationary. Second, there is a general increasing trend in the measured phase which is predicted by the model but with a slower rate of increase. Finally, the simulated phase values are lower than the measured values by 3°–6°. It must be mentioned here that the multilayered formulation only accounts for the dominant mode to exist

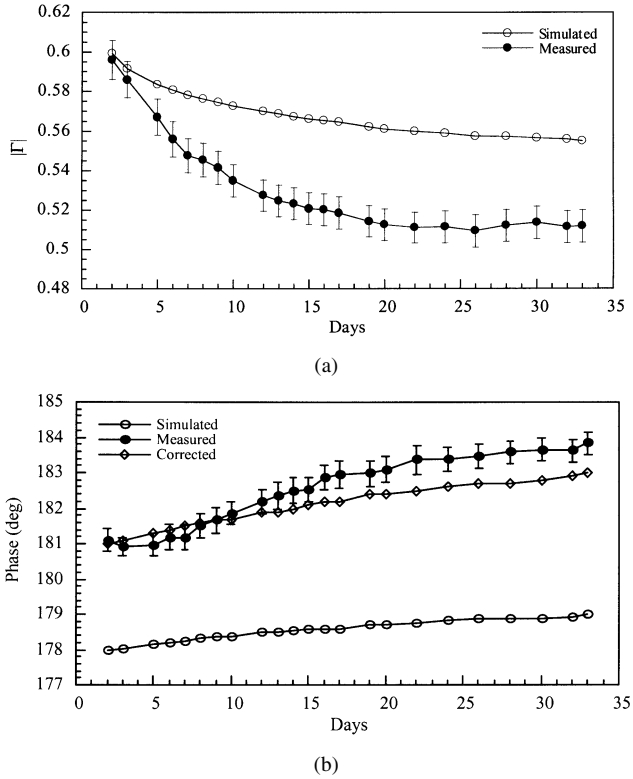

Fig. 6. Comparison between the simulated and measured (a) magnitude and (b) phase of reflection coefficient at 3 GHz for cycle 1 using the water content distribution shown in Fig. 5.

at the waveguide aperture [28]. However, any time there is a discontinuity in a waveguide or when an open-ended rectangular waveguide is terminated with another medium (i.e., the mortar cube) higher-order modes are also generated at the aperture of the waveguide in addition to the dominant mode [32], [34]. The measured results, however, inherently include the dominant modes as well. Using the multimode derivation in [32], which is for a rectangular waveguide radiating into a half-space of a dielectric material, it can be shown that the difference between the multilayered formulation and the measurements is between 3°–4° at 3 GHz and as a function of the dielectric properties of the cube [i.e., for the limiting cases of day 1 (the most moist) and the last day (the driest), and both represent the most homogeneous case of the mortar]. The same is true at 10 GHz and the phase difference can also be shown to be 2.4°–4°. Consequently, the simulated phase results were corrected for accordingly as shown in Fig. 6(b). Hereon, the corrected simulated phase results will be shown for the remaining figures. Finally, although the results of this model, using the water distribution functions shown in Fig. 5 did not match the measured results well, they showed very encouraging trends.

Further investigation revealed that to improve the model, it is not sufficient to consider only evaporation. Consequently, the water distribution functions were further modified to represent the movement of water through the cube during the drying cycle. The primary change involves the moving of the peaks into the cube as well as its widening, as a function of increasing days. The important fact is that the overall shape of the distributions still follows a Rayleigh-like function. The rate at which the shape of these curves was changed as well as the manner in

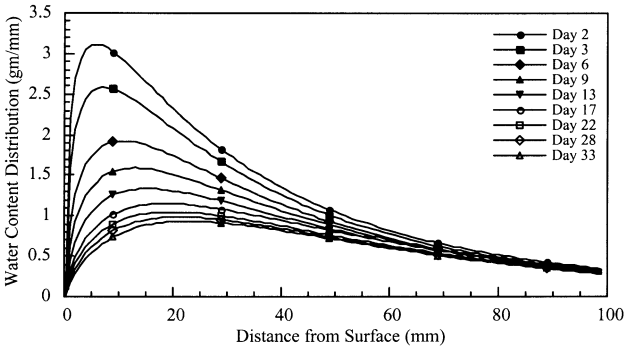

Fig. 7. Water content distribution obtained from the model, representing both evaporation and diffusion, for cycle 1.

which they did so on a day-to-day basis was determined from an extensive trial and error process, to determine the empirical factors, k_1, k_2, and k_3. The $\varepsilon_{\text{reff}}$ for each of the layers was then calculated based on the procedure mentioned earlier. This data was then fed into the multilayered formulation to simulate the reflection properties. The mismatch in the actual and simulated reflection properties was then used as a guiding factor to improve the model (i.e., refine k_1, k_2, and k_3). Fig. 7 shows the final water content distribution curves for several days of cycle 1. As shown, these distribution functions now represent both evaporation and water movement within the cube by noting that the peaks move toward the core of the cube and get broader as a function of increasing days. It is evident from the curves that although the evaporation from the surface and moisture movement through the cube occur concurrently, the process of evaporation is the dominating component; its dominance, however, diminishes as the water moves toward the core. The revised set of water distribution functions were subsequently used to produce the simulated $|\Gamma|$ and phase of reflection coefficient at 3 GHz, as shown in Fig. 8(a) and (b). The agreement between the simulated and measured $|\Gamma|$ clearly is very good and improved significantly compared to those shown in Fig. 6(a). The agreement between the simulated and measured phase is also very good. In addition, using the new distributions the dip in the measured phase behavior is clearly replicated by the model. Similarly, using the *same* water distribution functions the comparison between the simulated and measured $|\Gamma|$ and phase of reflection coefficient were obtained at 10 GHz (X-band), as shown in Fig. 9(a) and (b), respectively. The results show good agreement both in trend and values for these parameters. The simulated $|\Gamma|$ is higher than the measured $|\Gamma|$ during the early days of the cycle, with a maximum 7% difference at day 1. The simulated phase is also maximally different from the measured phase by $\sim 1^\circ$–2° during the same early days.

One of the model parameters that had to be determined was the depth at which the maximum amount of water exists in the drying cube. The empirical parameter k_1 in (1) is dependent on the depth into the cube and was determined by investigating the shape of the phase of reflection coefficient at 3 GHz. It was also observed that the depth at which the maximum amount of water existed had to be moved gradually on a daily basis so as to be able to simulate the shape of phase of reflection at 3 GHz. This movement however was found to gradually slow down as a function of increasing days of drying.

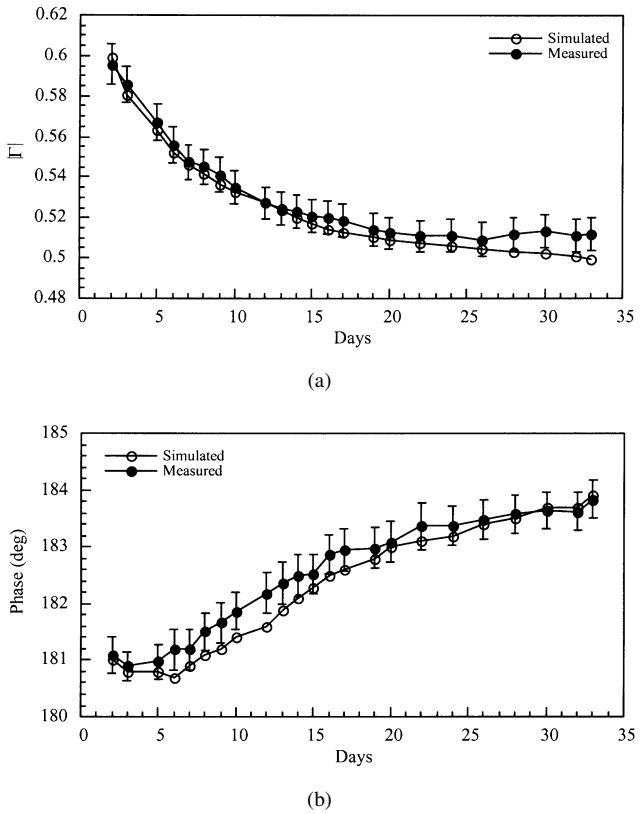

Fig. 8. Comparison between the simulated and measured (a) magnitude and (b) phase of reflection coefficient at 3 GHz for cycle 1 using the water content distribution shown in Fig. 7.

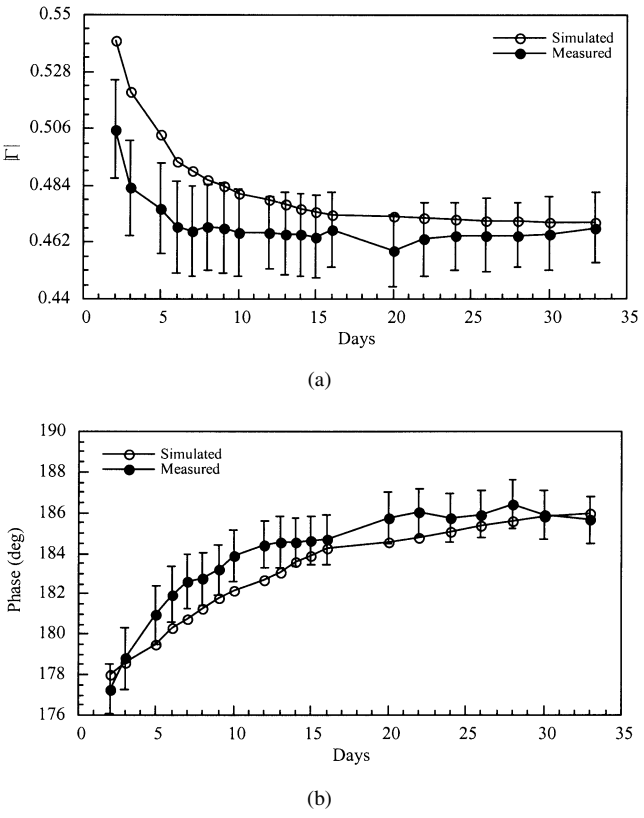

Fig. 9. Comparison between the simulated and measured (a) magnitude and (b) phase of reflection coefficient at 10 GHz for cycle 1 using the water content distribution shown in Fig. 7.

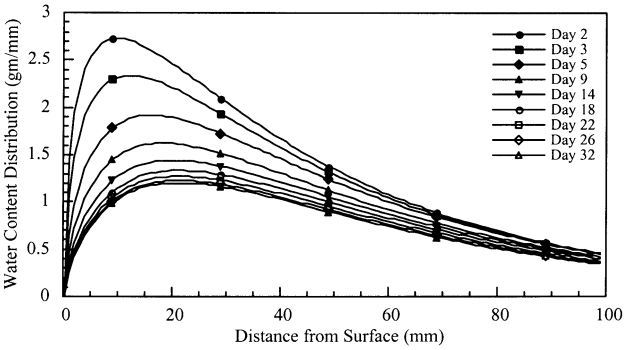

Fig. 10. Water content distribution obtained from the model for cycle 2.

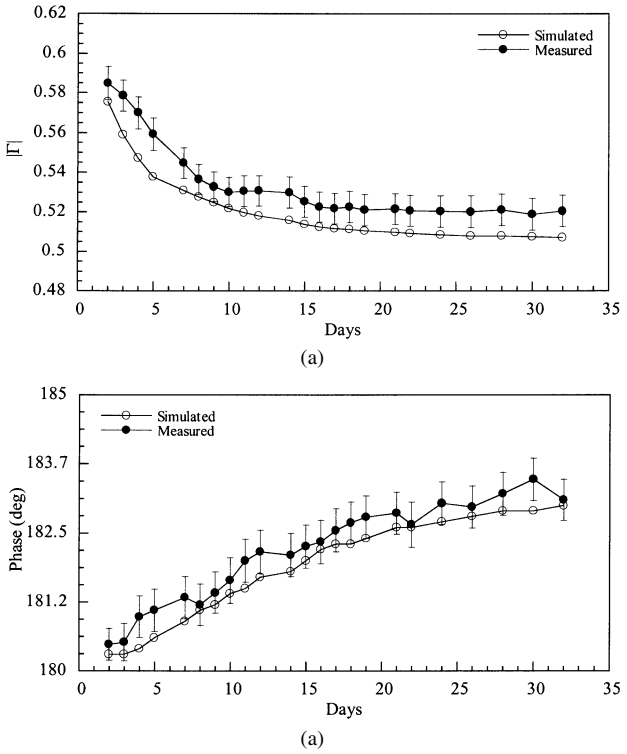

Fig. 11. Comparison between the simulated and measured (a) magnitude and (b) phase of reflection coefficient at 3 GHz for cycle 2.

B. Cycle 2

After obtaining satisfactory results for cycle 1, the simulation of cycle 2 was initiated. The step-by-step modeling process adopted for cycle 1 was again followed for these two cycles with a notable exception. At the end of cycle 1, there is a certain amount of residual water, absorbed during the first soaking cycle, which is distributed in the cube as shown by the distribution function for day 33 in Fig. 7 (i.e., the last day of cycle 1). Hence, when the cube is once again soaked, the additional amount of water that each layer takes in will be influenced by the residual water distribution in the cube. Consequently, the water distribution functions following the second cycle of soaking would be somewhat different than those in cycle 1. Thus, for cycle 2 the residual amount of water from cycle 1 should be added to the additional amount of water absorbed during the second soaking period, whereas for cycle 3, the residual amount of water from cycle 2 should be added to the additional amount of water absorbed during the third soaking cycle. Fig. 10 shows the resulting water distribution for cycle 2. Fig. 11 shows the simulation results at S-band (3 GHz) for cycle 2. The results show very good agreement between the simulated and the measured results. The simulation results at X-band (10 GHz) also showed good agreement with the measured reflection properties [31]. A notable difference between the reflection properties of cycles 1 and 2 is the shape of the phase of reflection coefficient at 3 GHz during the first few days of either cycle. Empirical parameter k_1 was found to be needed to be carefully chosen for the simulated phase shapes to follow the measured phase closely. The influence of choosing k_1 on the water distribution curves was that in comparison to cycle 1, for cycle 2, the point at which the maximum amount of water existed (for day one) moved toward the core by a few millimeters.

For cycle 3, the water distribution functions were obtained in the same manner as those for cycle 2 [31]. Once again, as compared to cycle 2 the point at which the maximum amount of water exists (for day one) was further moved toward the core by a few millimeters. The simulated and measured reflection properties were in good agreement at both frequency bands and have been omitted in the interest of brevity.

VI. Discussion

The simulation results, using the semiempirical electromagnetic model outlined in this paper, agreed well with the measured results for the magnitude and phase of reflection coefficient of the mortar cube at two different microwave frequencies. The model is based on a discrete approach for evaluating the reflection properties of layered dielectric materials. Choice of several parameters requires further discussion as follows.

Considering the fact that the evaporation of water from the cube did not take place in a uniform fashion from all sides, a factor of 5 (instead of 6) was chosen to determine the equivalent degree of evaporation from each side of the cube. Since evaporation and water movement occur in the cube under test, ample consideration was given before this factor was arrived at, as discussed in Section IV-B. It is important to note that if instead of a cube a different geometry had been chosen then this factor would be different. Similarly, if the mortar under test had only been exposed to air from one side, as would be the case of a pavement or roadway, this factor would have been different as well. Therefore, this geometry dependent parameter can also be viewed as another empirical parameter of this model for more complex geometries.

Given the dielectric properties of the mortar cube and the incident microwave power coupled into the mortar, the expected depth of penetration was estimated to be no more than 100 mm. Considering the fact that the mortar was soaked for 20 h, the water content at this depth is not expected to be relatively large (as also shown by the water distribution functions). Therefore, the consideration of using a maximum of 100 mm in the model is a reasonable one since the contribution to the magnitude and phase of reflection coefficient from 80–100 mm are negligible. This fact was tested by running the model using shallower depths, but well beyond the water distribution peak locations, and the influence on the outcome of the model was, indeed, negligible. In one experiment, a similar mortar cube was soaked in a similar manner and then immediately broken to visually inspect the depth to which the water had soaked. This depth was determined to be approximately 60 mm. This

observation and the water content distribution functions for the three cycles, past approximately 60-mm deep in the cube are in good agreement. For a mortar cube that may be soaked for a longer period this depth may vary. However, the model is versatile enough to account for this fact.

One would wonder whether the water distribution functions that are obtained from this model are unique or some other distribution function may also yield similar reflection coefficient results. The current model has been capable of simulating four independent parameters (magnitude and phase of reflection coefficient at two frequency bands) quite well for three different cycles. As explained in Section IV-B, several other distribution functions were also used with very disappointing results. It was also shown that the temporal movement of the water content peak and its widening (representing water movement within the cube) was a crucial issue for the success of the current model. Also, there is no multiple scattering involved in the measurement process. Therefore, it is expected that the water content distribution functions obtained from this model very closely describe the actual water distribution and its temporal variation in the cube. It is also important to note that the water distribution functions obtained from the initial model mentioned in Section IV-A and the current model described in Section IV-B displayed similar water movement characteristic within the cube. The two modeling processes were independent of one another and yet the results showed significant similarity in the temporal water distribution behavior [31]. Finally, it is of utmost importance to note that the resulting water distribution functions for all cycles, but in particular for cycle 1, were capable of simulating the dip in the early days of the phase behavior at 3 GHz. Extensive investigation showed that only these curves are capable of predicting this dip. However, what makes these curves unique is the fact that the same distribution functions also properly predicted the phase behavior at 10 GHz, which does not have such a dip.

The porosity of similar mortar cubes has been estimated to be between 7%–10% [11], [12]. Using the process outlined in the modeling section, the porosity of the cube was determined to be $\sim$8%. The assumption made here was that the 1-mm-thick layer with the most water content should be saturated. This is a reasonable assumption. However, even if this layer is not fully saturated but only 90% saturated, the resulting porosity (i.e., 7.2%), once combined with calculating the effective dielectric properties of the layer using a dielectric mixing model, will not significantly affect the final model outcome.

All of the above considerations must be put in light of the fact that measured results were averaged over four sides of the cube. The simulated results agreed well with the average measured results. Any sensitivity that the model may have with respect to the parameters mentioned in this section could be construed as variations about the mean.

VII. Conclusion

The foundation and the results of a semiempirical model, simulating the microwave reflection properties of mortar exposed to cyclical episodes of soaking in distilled water and drying, at two distinct frequencies were presented. Overall, the results of the model agreed quite well with the measured results. The most important outcome of the model is the temporal water content distribution inside the mortar cube for three successive soaking and drying cycles. The distribution functions followed a well-known behavior (Rayleigh-like) and its specific parameters were determined empirically. The resulting water content distribution functions can be used to evaluate water content at any depth in the mortar and for any day of any cycle indicating the movement of water due to evaporation and diffusion. Moreover, these distribution functions account for both evaporation of water and movement of water both toward the core of the cube and toward the surface of the cube. It is this fact that enabled the model to correctly simulate the dip in the phase of reflection coefficient at 3 GHz during the first few days of the cycle 1. The model is also versatile to account for variations in the manner the mortar sample was exposed to water and the geometry of the sample. The model also provides for evaluating water distribution in the cube with sub-millimeter spatial resolution if need be (i.e., 1-mm resolution was used here).

The water distribution functions obtained from this model can ultimately be used to determine many important properties of cement-based materials, including the distribution and total amount of chloride ions. This particular application is currently a focus of this ongoing investigation.

References

[1] S. D. Beyea, B. J. Balcom, T. W. Bremner, P. J. Prado, D. P. Green, R. L. Armstrong, and P. E. Grattan-Bellow, "Magnetic resonance imaging and moisture content profiles of drying concrete," *Cement Concrete Res.*, vol. 28, no. 3, pp. 453–463, 1998.

[2] M. Kuntz and P. Lavallee, "Experimental evidence and theoretical analysis of anomalous diffusion during water infiltration in porous building materials," *J. Phys. D: Appl. Phys.*, vol. 34, pp. 2547–2554, 2001.

[3] K. Hong and R. D. Hooton, "Effects of cyclic chloride exposure on penetration of concrete cover," *Cement Concrete Res.*, vol. 29, pp. 1379–1386, 1999.

[4] O. M. Jensen, P. F. Hansen, A. M. Coats, and F. P. Glasser, "Chloride ingress in cement paste and mortar," *Cement Concrete Res.*, vol. 29, pp. 1497–1504, 1999.

[5] W. J. McCarter, "Monitoring the influence of water and ionic ingress on cover-zone concrete subjected to repeated absorption," *Cement, Concrete Aggregates*, vol. 18, pp. 55–63, 1996.

[6] H. Hashida, K. Tanaka, and M. Koike, "Moisture distribution in concrete before and after application of the finish," *Build. Res. Practice*, vol. 18, no. 5, pp. 303–308, 1990.

[7] G. E. Monfore, "A review of methods for measuring water content of highway components in place," *Highway Res. Records*, no. 342, pp. 17–26, 1971.

[8] R. Zoughi, S. Gray, and P. S. Nowak, "Microwave nondestructive estimation of cement paste compressive strength," *ACI Mater. J.*, vol. 92, no. 1, pp. 64–70, Jan.–Feb. 1995.

[9] W. Shalaby and R. Zoughi, "Analysis of monopole sensors for cement paste compressive strength estimation," *Res. Nondestruct. Eval.*, vol. 7, no. 2/3, pp. 101–105, 1995.

[10] K. Mubarak, K. J. Bois, and R. Zoughi, "A simple, robust and on-site microwave technique for determining water-to-cement (w/c) ratio of fresh portland cement-based materials," *IEEE Trans. Instrum. Meas.*, vol. 50, pp. 1255–1263, Oct. 2001.

[11] K. Bois, R. Mirshahi, and R. Zoughi, "Dielectric mixing models for cement based materials," in *Proc. Rev. Progr. Quantitative Nondestructive Evaluation*, 1997, vol. 16A, pp. 657–663.

[12] K. Bois, A. Benally, P. S. Nowak, and R. Zoughi, "Microwave nondestructive determination of sand to cement (s/c) ratio in mortar," *Res. Nondestruct. Eval.*, vol. 9, no. 4, pp. 227–238, 1997.

[13] A. Joisel, K. J. Bois, A. D. Benally, R. Zoughi, and J. C. Bolomey, "Embedded modulated dipole scattering for near-field microwave inspection of concrete: preliminary investigation," in *Proc. SPIE Subsurf. Sens. Applicat. Conf.*, vol. 3752, Denver, CO, July 18–23, 1999, pp. 208–214.

[14] K. Bois, A. Benally, and R. Zoughi, "Microwave near-field reflection property analysis of concrete for material content determination," *IEEE Trans. Instrum. Meas.*, vol. 49, pp. 49–55, Feb. 2000.

[15] K. J. Bois, A. D. Benally, P. S. Nowak, and R. Zoughi, "Cure-state monitoring and water-to-cement ratio determination of fresh portland cement based materials using near field microwave techniques," *IEEE Trans. Instrum. Meas.*, vol. 47, pp. 628–637, June 1998.
[16] K. Bois and R. Zoughi, "A decision process implementation for microwave near-field characterization of concrete constituent makeup," *Spec. Issue Subsurf. Sens. Technol. Applicat.: Adv. Applicat. Microwave Millim. Wave Nondestruct. Eval.*, vol. 2, no. 4, pp. 363–376, Oct. 2001.
[17] S. Kharkovsky, M. Akay, U. Hasar, and C. Atis, "Measurement and monitoring of microwave reflection and transmission properties of cement-based specimens," in *Proc. IEEE Instrumentation and Measurement Technology Conf.*, Budapest, Hungary, May 21–23, 2001, pp. 513–518.
[18] K. Bois, H. Campbell, A. Benally, P. S. Nowak, and R. Zoughi, "Microwave noninvasive detection of grout in masonry," *Masonry J.*, vol. 16, no. 1, pp. 49–54, June 1998.
[19] D. Hughes, M. Kazemi, K. Marler, J. Myers, R. Zoughi, and T. Nanni, "Microwave detection of delamination between fiber reinforced polymer (FRP) composites and hardened cement paste," in *Proc. 28th Annu. Rev. Progr. Quantitative Nondestructive Evaluation*, vol. 21, Brunswick, ME, July 29–Aug. 3 2001, pp. 512–519.
[20] J. Li and C. Liu, "Noncontact detection of air voids under glass epoxy jackets using a microwave system," *Spec. Issue Subsurf. Sens. Technol. Applicat.: Adv. Applicat. Microwave Millim. Wave Nondestruct. Eval.*, vol. 2, no. 4, pp. 411–423, Oct. 2001.
[21] K. Bois, A. Benally, and R. Zoughi, "Near-field microwave noninvasive determination of NaCl in mortar," in *Proc. Inst. Elect. Eng.*, vol. 148, July 2001, pp. 178–182.
[22] C. Hu, A. Benally, T. Case, R. Zoughi, and K. Kurtis, "Influence on the near-field microwave reflection properties of chloride in mortar specimens made of cement types II, III and V at X and S bands," in *Proc. SPIE Conf.*, vol. 4129, San Diego, CA, July 30–Aug. 4 2000, pp. 31–38.
[23] C. Hu, T. Case, M. Castle, R. Zoughi, and K. Kurtis, "Microwave evaluation of accelerated chloride ingress in mortar," in *Proc. 27th Annu. Rev. Progr. Quantitative Nondestructive Evaluation*, vol. 20A, Ames, IA, July 17–21, 2000, pp. 467–473.
[24] J. Case, R. Zoughi, K. Donnell, D. Hughes, and K. E. Kurtis, "Microwave analysis of mortar prepared with type I/II, III and V cement and subjected to cyclical chloride exposure," in *Proc. 28th Annu. Rev. Progr. Quantitative Nondestructive Evaluation*, vol. 21, Brunswick, ME, July 29–Aug. 3 2001, pp. 498–505.
[25] S. Peer, J. Case, K. Donnell, D. Hughes, R. Zoughi, and K. E. Kurtis, "Investigation of microwave reflection properties of mortar exposed to wet-dry cycles of tap water and chloride bath," in *Proc. 28th Annu. Rev. Progr. Quantitative Nondestructive Evaluation*, vol. 21, Brunswick, ME, July 29–Aug. 3 2001, pp. 1269–1276.
[26] R. Zoughi, S. Peer, J. Case, E. Gallaher, and K. E. Kurtis, "Microwave near-field evaluation of the effects of cyclical chloride exposure and compressive loading on mortar," in *Proc. 3rd Int. Workshop Structural Health Monitoring (IWSHM)*, Stanford, CA, Sept. 12–14, 2001, pp. 575–583.
[27] S. Peer, J. T. Case, E. Gallaher, K. E. Kurtis, and R. Zoughi, "Microwave reflection and dielectric properties of mortar subjected to compression force and cyclically exposed to water and sodium chloride solution," *IEEE Trans. Instrum. Meas.*, vol. 52, p. 111, Feb. 2002.
[28] S. Bakhtiari, S. Ganchev, N. Qaddoumi, and R. Zoughi, "Microwave noncontact examination of disbond and thickness variation in stratified composite media," *IEEE Trans. Microwave Theory Tech.*, vol. 42, pp. 389–395, Mar. 1994.
[29] V. Kraszewski, *Microwave Aquametry*. New York: IEEE Press, 1996, ch. 9.
[30] F. T. Ulaby, R. K. Moore, and A. K. Fung, *Microwave Remote Sensing: Active and Passive*. Dedham, MA: Artech House, 1986, vol. 3, pp. 2017–2025.
[31] S. Peer, "Nondestructive Evaluation of Moisture and Chloride Ingress in Cement-Based Materials Using Near-Field Microwave Techniques," M.S. thesis, Elect. Comput. Eng. Dept., Univ. Missouri-Rolla, Rolla, MO, Dec. 2002.
[32] K. Bois, A. Benally, and R. Zoughi, "An exact multimode solution for the reflection properties of an open-ended rectangular waveguide radiating into a dielectric half-space: forward and inverse problems," *IEEE Trans. Instrum. Meas.*, vol. 48, pp. 1131–1140, Dec. 1999.
[33] A. Sihvola, "Electromagnetic mixing formulas and applications," *Inst. Elect. Eng. Electromagn. Ser. 47*, 1999.
[34] C. Huber, H. Abiri, S. Ganchev, and R. Zoughi, "Modeling of surface hairline crack detection in metals under coatings using open-ended rectangular waveguides," *IEEE Trans. Microwave Theory Tech.*, vol. 45, pp. 2049–2057, Nov. 1997.

Shanup Peer (M'01) received the B.Tech. degree in electrical and electronics engineering from the University of Kerala, India, in 1999 and the M.S degree in electrical engineering from the University of Missouri-Rolla (UMR), Rolla, in 2002.

Since 2000, he has been a Graduate Research Assistant with the Applied Microwave Nondestructive Testing Laboratory (AMNTL), Electrical and Computer Engineering Department, UMR. His current research involves the evaluation of moisture and chloride ingress in cement-based material based on microwave nondestructive techniques.

Kimberly E. Kurtis received the B.S.E. degree in civil engineering from Tulane University, New Orleans, LA, and the M.S and Ph.D degrees in civil engineering from the University of California, Berkeley.

She is an Assistant Professor with the School of Civil and Environmental Engineering, Georgia Institute of Technology, Atlanta. She is an Associate Editor for the *ASCE Journal of Materials in Civil Engineering*. She is the Chairman of the ACI Committees E802: Teaching Methods and Educational Materials and a member of ACI Committee 201: Durability and 236: Materials Science of Concrete, as well as TRB Committee A2E01: Durability. Her area of research is in construction materials, with a strong emphasis on the microstructure and durability of cement-based materials.

Reza Zoughi (SM'93) received the B.S.E.E, M.S.E.E, and Ph.D. degrees in electrical engineering (radar remote sensing, radar systems, and microwaves) from the University of Kansas, Lawrence.

From 1981 to 1987, he was with the Radar Systems and Remote Sensing Laboratory (RSL), University of Kansas. Currently, he is the *Schlumberger Distinguished Professor* of electrical and computer engineering at the University of Missouri-Rolla (UMR), Rolla. Prior to joining UMR in January 2001, he was with the Electrical and Computer Engineering Department, Colorado State University (CSU), Fort Collins, which he joined in 1987 and where he was a Professor. He held the position of *Business Challenge Endowed Professor* of electrical and computer engineering from 1995 to 1997 while at CSU. He has given numerous invited talks on the subject of microwave nondestructive testing and evaluation. He is an Associate Technical Editor for *Materials Evaluation*, and he has served as the Guest Associate Editor for the Special Microwave NDE Issue of *Research in Nondestructive Evaluation* and co-Guest editor for the Special Issue of *Subsurface Sensing Technologies and Applications: Advances and Applications in Microwave and Millimeter Wave Nondestructive Evaluation* in 1995. He served as the *Research Symposium Co-Chair for the American Society for Nondestructive Testing (ASNT) Spring Conference and 11th Annual Research Symposium*, Portland, OR, March 2002. He has to his credit over 300 journal publications, conference proceedings and presentations, technical reports, and overview articles. He is also the author of a graduate textbook entitled *Microwave Nondestructive Testing and Evaluation Principles* (Norwell, MA: Kluwer, 2000) and co-Author with A. Bahr and N. Qaddoumi of a chapter on microwave techniques in an undergraduate introductory textbook entitled *Nondestructive Evaluation: Theory, Techniques, and Applications* edited by P.J. Shull (New York: Marcel–Dekker, 2002). In addition, he has seven patents to his credit, all in the field of microwave nondestructive testing and evaluation. His current areas of research include developing new nondestructive techniques for microwave and millimeter wave inspection and testing of materials (NDT), developing new electromagnetic probes to measure characteristic properties of material at microwave frequencies, and developing embedded modulated scattering techniques for NDT purposes in particular for complex composite structures.

Dr. Zoughi is a member of Sigma Xi, Eta Kappa Nu, and the American Society for Nondestructive Testing (ASNT). He has received two Outstanding Teaching Commendations and an Outstanding Teaching Award (for the 2002–2003 academic year) from UMR. He was voted the most outstanding teaching faculty seven times by the junior and senior students at the Electrical and Computer Engineering Department, CSU. He received the College of Engineering Abell Faculty Teaching Award in 1995. He is the 1996 recipient of the Colorado State Board of Agriculture Excellence in Undergraduate Teaching Award. He was recognized as an honored researcher for seven years by the Colorado State University Research Foundation. He is an Associate Technical Editor for the IEEE TRANSACTIONS ON INSTRUMENTATION AND MEASUREMENT. He served as the Technical Chair for the *IEEE Instrumentation and Measurement Technology Conference* (IMTC), Vail, CO, May 2003. He is also the Guest Editor for the Special Issue of the IEEE TRANSACTIONS ON INSTRUMENTATION AND MEASUREMENT on IMTC 2003.